

In Vivo Laser-Tissue Interactions and Healing Responses From 20- vs 100-Millisecond Pulse Pascal Photocoagulation Burns

Mahiul M. K. Muqit, MRCOphth; Jane C. B. Gray, RMIP; George R. Marcellino, PhD; David B. Henson, PhD; Lorna B. Young, MBChB; Niall Patton, FRCOphth; Stephen J. Charles, FRCOphth; George S. Turner, FRCOphth; Andrew D. Dick, FMedSci; Paulo E. Stanga, MD

Objectives: To compare in vivo burn morphologic features and healing responses of Pascal 20- and 100-millisecond panretinal photocoagulation (PRP) burns in proliferative diabetic retinopathy.

Design: Prospective randomized controlled trial with 24 eyes assigned to either 20- or 100-millisecond Pascal PRP. Fundus autofluorescence and Fourier domain optical coherence tomography (FD-OCT) were performed 1 hour and 2 and 4 weeks after treatment. Main outcome measures included burn morphologic features on FD-OCT and greatest linear diameter (GLD) of laser burns as evaluated in 6 standard Early Treatment of Diabetic Retinopathy Study photographic fields using autofluorescence.

Results: The contemporaneous increase in autofluorescence is observed with increasing pulse duration. Differences in mean GLD between 100- and 20-

millisecond burns were 63 μm at 1 hour and 198 μm at 4 weeks ($P < .001$ for both). At 4 weeks, all burns corresponded to defects at the junction of inner and outer segments of photoreceptors (JI/OSP) and apical retinal pigment epithelium. After 4 weeks, the GLD of 20-millisecond burns reduced significantly by 35% ($P < .001$), with no change in 100-millisecond burns.

Conclusions: All burns initially appear as equivalent square-edged, columnar foci of hyperreflectivity in the outer retina. Pascal 20-millisecond burns progressively reduce in size, and this suggests a novel healing response localized to the JI/OSP and apical retinal pigment epithelium. The higher-fluence 100-millisecond burns develop larger defects due to thermal blooming and collateral damage.

Arch Ophthalmol. 2010;128(4):448-455

LASER PANRETINAL PHOTOCOAGULATION (PRP) standards for treating proliferative diabetic retinopathy (PDR) were established by the Early Treatment of Diabetic Retinopathy Study (ETDRS) Study Group more than 20 years ago.¹ More recently, clinical investigators have examined the effects of millisecond, microsecond, and subnanosecond pulse-duration laser photocoagulation techniques.²⁻⁴

Visible end point PRP remains the criterion standard for first-line PDR treatment.¹ Patients with sight-threatening PDR may require multiple laser treatments during their lifetime, and laser burn expansion is a well-recognized phenomenon.⁵ The aim of new laser technology is to achieve retinal photocoagulation that allows for the development of healing responses by selectively targeting the retinal pigment epithelium (RPE), with minimal photoreceptor loss and subsequent photoreceptor and RPE cell repopulation.⁶ However, a leading hypothesis is

that PRP works by inducing retinal cell death, thereby decreasing the cell signaling that causes neovascularization. A possible weakness of newer laser technology that performs a potentially minimally damaging treatment may be the lack of long-term therapeutic effects, as demonstrated by the 100-millisecond pulse-duration laser studies.

Autofluorescence imaging of photocoagulation burns has been reported after selective retinal therapy.⁷ Autofluorescence signals after selective retinal therapy are known to result in localized lack of autofluorescence after 1 hour, which later becomes hyperautofluorescent for up to 3 years. Patterns of autofluorescence may reflect the thermal reactions of laser at the level of the RPE, with variations in heat diffusion associated with a medium pulse compared with conventional longer-duration burns.⁸

The Pascal (Pattern Scanning Laser) Photocoagulator (OptiMedica Corp, Santa Barbara, California) was introduced in 2005 for retinal photocoagulation.⁹ It semi-automates the procedure using a brief pulse

Author Affiliations: Royal Eye Hospital, University of Manchester (Mr Muqit and Drs Henson and Stanga) and Manchester Royal Eye Hospital (Messrs Patton, Charles, and Turner; Ms Gray, and Dr Young), Manchester, England; OptiMedica Corp, Santa Clara, California (Dr Marcellino); and Bristol Eye Hospital, Bristol, England (Dr Dick).

duration combined with rapid raster scan application of multiple spots that allows shorter treatment delivery times. There may be less outer retina and RPE damage due to less collateral thermal diffusion.⁸

Histopathologic descriptions of photocoagulation burns have shown localization of laser lesions in the outer retina.^{4,8-10} Localization to the outer retina has been shown in less intense lesions with shorter pulse durations.⁸ Longer pulse durations and more intense lesions result in damage to the inner and outer retinal layers, likely due to thermal diffusion.¹⁰ Stanga et al¹¹ used scanning laser ophthalmoscope autofluorescence and time-domain optical coherence tomography (OCT) to assess the function of subfoveally translocated full-thickness RPE-choroid grafts in patients with age-related macular degeneration.

In a previous study¹² also undertaken at Manchester Royal Eye Hospital, 20-millisecond laser PRP was compared with 100-millisecond pulse-duration PRP in 22 eyes. The experience described herein in humans demonstrated that a shorter pulse duration required a higher power to achieve the desired therapeutic lesion. There was a highly significant difference in the mean power used between conventional 100-millisecond laser (235 mW) and Pascal 20-millisecond laser (396 mW) ($P < .001$). This first study¹² was retrospective and nonstandardized, and imaging of laser lesions was not performed. The present study contributes more detail regarding the morphologic features of laser lesions and fluence at different pulse durations in PDR in a prospective randomized controlled trial setting.

This is, to our knowledge, the first randomized clinical trial to investigate laser tissue-healing responses between Pascal 20-millisecond and standard-pulse 100-millisecond lasers by comparing the sequential findings in autofluorescence based on OCT findings. We describe the healing responses of laser burns in patients who underwent single-spot Pascal 100-millisecond PRP and multispot pattern Pascal 20-millisecond PRP. The primary objective was to study burn morphologic features of 20- and 100-millisecond laser lesions as visualized by means of Fourier domain OCT (FD-OCT) and autofluorescence.

METHODS

Patients who required PRP for newly diagnosed PDR were prospectively studied. The study protocol received ethics committee approval from Stockport Research Ethics Committee, and written informed consent was obtained from all of the patients.

STUDY POPULATION

No previous ophthalmic laser, medical, or surgical treatment had been performed in any patient. The randomization procedure involved sequentially numbered, opaque, sealed envelopes. The investigators and patients were unmasked to the treatment groups. All of the patients were recruited consecutively at a single site according to the study criteria. Patients underwent either unilateral or bilateral PRP according to randomization treatment allocation. In cases of bilateral study eye eligibility, the right eye was randomized first with treatment allocation, followed by left eye randomization and allocation.

Twenty-four eyes of 15 patients were included; no eyes were lost to follow-up.

The study inclusion criteria were as follows: older than 18 years; male or female patients with diabetes mellitus type 1 or type 2 who met the World Health Organization or American Diabetes Association criteria for diabetes; ETDRS visual acuity of 35 to 85 letters (Snellen equivalent of $\geq 6/60$); newly diagnosed PDR; mean retinal thickness in the central subfield of less than 300 μm as measured using OCT, with the absence of intraretinal or subretinal fluid; adequate pupil dilatation and clear media to perform laser photocoagulation, digital photography, and OCT; and the ability to perform an accurate Humphrey visual field test. The exclusion criteria were as follows: recent (previous 6 months) or ongoing poor glycemic control (hemoglobin A_{1c} 10%); uncontrolled hypertension (blood pressure $\geq 180/110$ mm Hg); history of chronic renal failure or renal transplantation for diabetic nephropathy; lens opacity or cataract that could affect vision and results; any previous surgical or laser treatment to either eye; planned YAG peripheral iridotomy; previous laser photocoagulation or macular laser treatment to either eye; a history of diabetic macular edema in either eye; any previous ocular condition that may be associated with a risk of macular edema; active eyelid or adnexal infection; previous retinal treatment (laser, drug, or surgery); and planned intraocular surgery within 1 year.

PROCEDURES

All of the patients underwent slitlamp biomicroscopy and fundus fluorescein angiography. Fundus photography, FD-OCT, and autofluorescence were performed at baseline and 1 hour, 2 weeks, and 4 weeks after laser photocoagulation.

PASCAL LASER PHOTOCOAGULATION SYSTEM

This is a frequency-doubled Nd:YAG solid-state laser with a wavelength of 532 nm. Photocoagulation is applied in a rapid pattern array with a pulse duration of 20 milliseconds.¹² We used a Mainster 165 PRP lens (Ocular Instruments Inc, Bellevue, Washington) in all cases, and a single investigator (M.M.K.M.) performed all the laser lesions. Twelve eyes underwent Pascal 20-millisecond PRP using 5 × 5 and 4 × 4 multispot arrays (20MS-PRP), and 12 eyes underwent Pascal 100-millisecond PRP using single-spot mode (100SS-PRP). In both groups, threshold laser photocoagulation treatment was titrated to and designated by a gray-white burn according to ETDRS guidelines for scatter argon photocoagulation. Fifteen hundred photocoagulation burns composed a full PRP treatment course in both groups using 400- μm laser spot sizes at the retina placed 1.5 burn widths apart.

FUNDUS AUTOFLUORESCENCE

Intensities of autofluorescence are determined by the quantity and distribution of lipofuscin.¹³ A fundus flash camera system (TRC-50DX [Type IA]; Topcon Instruments, Newbury, England) was used. The autofluorescence exciter filter placed in the illumination path has a central wavelength of 580 nm and a bandwidth of 30 nm (60% transmission). The autofluorescence barrier filter, placed in the viewing path, has a central wavelength of 695 nm and a bandwidth of 40 nm. The autofluorescence image shows the spatial distribution of autofluorescence.¹⁴

FOURIER DOMAIN OCT

In FD-OCT (3D OCT-1000; Topcon Instruments), image detection is based on the retrieval of optical A-scans from inter-

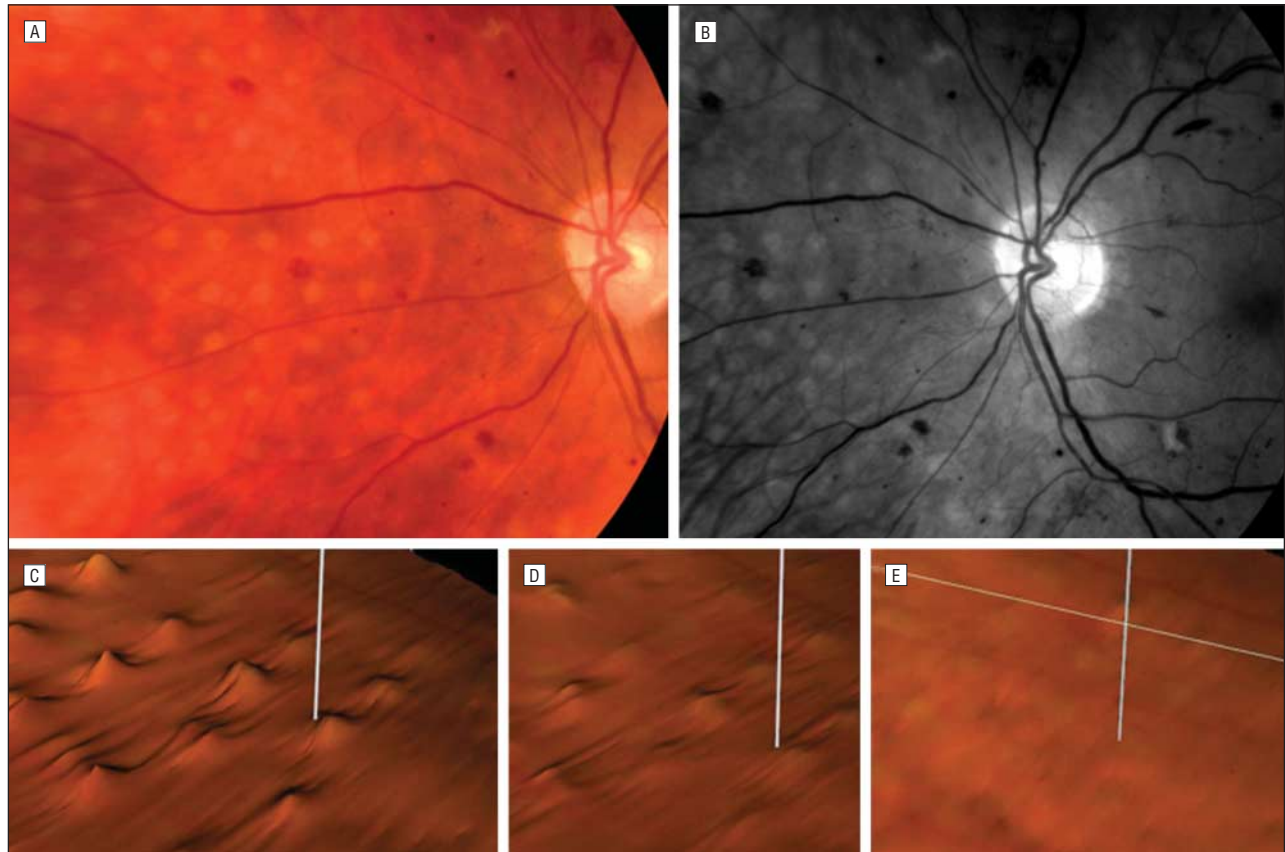


Figure 1. Imaging of gray-white visible Pascal 20-millisecond treatment burns at 1 hour (400- μ m spot size, 5 \times 5 array, and 1.5 burn width spacing). Color (A) and red-free (B) fundus photographs were taken and Fourier domain optical coherence tomography 3-dimensional scans map the laser burn-induced reflectivity alterations to the junction of inner and outer segments of photoreceptors (C) and the apical retinal pigment epithelium (RPE) layer (D), with no visible alteration in reflectivity at the level of the basal aspect of the RPE (E).

ferometric signals as a function of the spectral fringe pattern.¹⁵ Important reflective signals include the inner highly reflective layer (HRL), which corresponds to the interface between the vitreous and the internal limiting membrane, and the outer HRL, which is in the outer retina. The thin band of high reflectivity immediately internal to the outer HRL is believed to correspond to the junction between the inner and outer segments of the photoreceptors (JI/OSP), and the outer HRL has been reported to represent the melanin in RPE.¹¹ We used 6 \times 6-mm retina 3D scans combined with overlapping line scans to visualize laser burns in detail. We examined the reflectivity signals of 50 laser lesions in each nasal OCT field and 3600 lesions in total were analyzed over time.

ASSESSMENT OF LASER BURNS

Six standard ETDRS photographic fields were taken for fundus photography and autofluorescence imaging. The greatest linear diameter (GLD) of a laser burn (20MS-PRP and 100SS-PRP) was measured using autofluorescence images with the GLD passing through the center of each laser burn. Autofluorescence images were superior to color and red-free fundus images for measurement of the GLD, as medium-pulse 10- to 20-millisecond laser lesions have previously been shown to be accurately delineated on autofluorescence images across time.¹⁶ An average GLD was calculated from 150 photocoagulation spots visualized using autofluorescence (25 burns in each of 6 ETDRS fields). Mean GLDs were recorded for both groups at 1 hour and were compared with the GLD at the 4-week time point. The morphologic features of laser burns were evaluated using

FD-OCT in the nasal quadrant of the retina. A 2-tailed *t* test was used to explore differences in laser power and GLD between both groups, and the null hypothesis was rejected for $P < .05$.

RESULTS

Twenty-four eyes with completed follow-up were studied. The mean (SD) power used for 20MS-PRP was significantly higher at 266 (86.5) mW (range, 200-456 mW; $P < .001$) compared with that used for 100SS-PRP (140 [22.2] mW; range, 104-188 mW). The mean fluence for 20MS-PRP was 4.2 J/cm² (range, 3-7 J/cm²), and this was significantly lower than that used for 100SS-PRP (11.2 J/cm²; range, 8-15 J/cm²; $P < .001$).

Autofluorescence demonstrated lack of autofluorescence 1 hour after laser, and the immediate burn morphologic features were similar for both pulse durations. One-hour FD-OCT demonstrated vertical bands of moderate and high reflectivity in the outer nuclear layer, with extension from the inner HRL through the outer plexiform layer. These bands corresponded to 20- and 100-millisecond photocoagulation burns (**Figure 1** and **Figure 2**). The outer plexiform layer showed thickening at the base of the vertical bands, with disruption at the apical RPE. At all pulse durations, the outer border of the outer HRL showed no signs of disruption, and there were no clinical signs of intraretinal or subretinal hemorrhage.

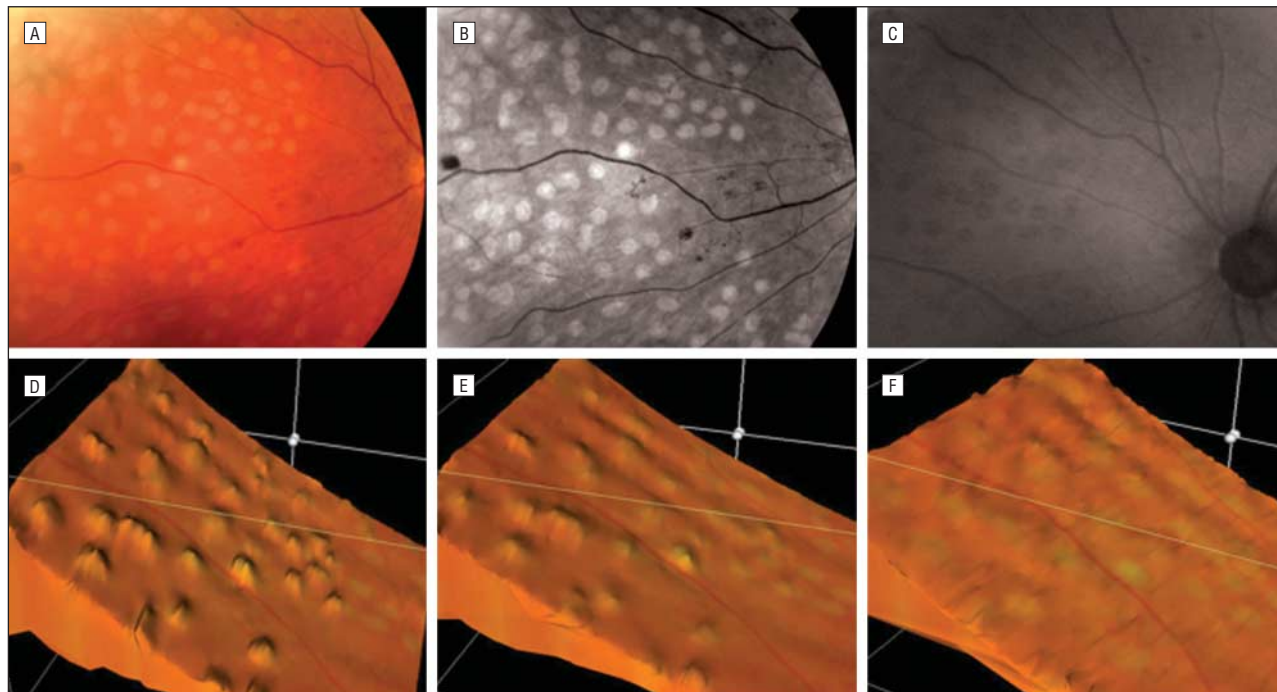


Figure 2. Imaging of gray-white visible Pascal 100-millisecond treatment burns at 1 hour (400- μm spot size). Color (A) and red-free (B) fundus photographs show threshold laser burns. C, Laser burns are demonstrated as spots lacking autofluorescence in the nasal retina. Three-dimensional Fourier domain optical coherence tomography at 1 hour through a single row of Pascal 100-millisecond burns map the laser burn–induced reflectivity alterations to the junction between the inner and outer segments of the photoreceptors (D) and the apical retinal pigment epithelium (RPE) layer (E), with no visible alteration in reflectivity at the level of the basal aspect of the RPE (F). White grid lines demonstrate the exact alignment of the retinal layers during 3-dimensional software analysis of the horizontal optical coherence tomography scans.

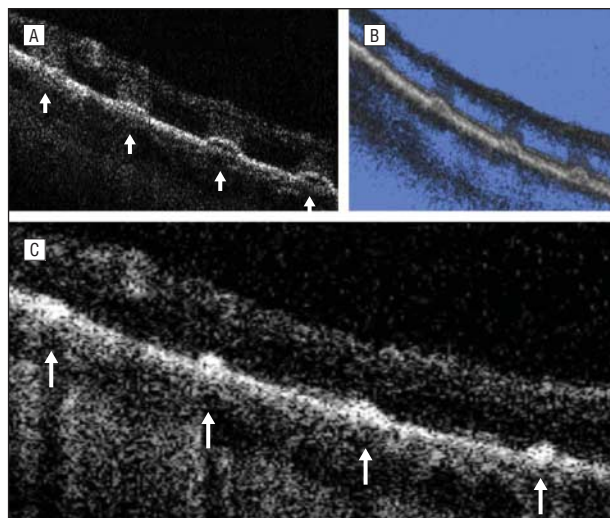


Figure 3. Horizontal Fourier domain optical coherence tomography at 1 hour through a single row of Pascal 20-millisecond burns in the nasal retina (arrow) shows 4 vertical bands of increased optical reflectivity in the outer plexiform layer (OPL) extending through the junction between the inner and outer segments of the photoreceptors and into the apical surface of the retinal pigment epithelium (RPE). A, The Pascal burns at 1 hour may be graded, starting from the far left, as follows: the outer highly reflective layer (HRL) remains intact, with foci of reduced reflectivity in the outer HRL; diffuse disruption and thickening of the outer HRL; hyporeflexive splitting of the outer HRL, with compression of the vertical band of reflectivity in the OPL/outer nuclear layer (ONL); and a bleb of reduced optical reflectivity is present in the outer HRL, with elevation of the inner aspect and a triangular band of hyperreflectivity in the OPL/ONL. B, Three-dimensional scan shows localization of columnar-shaped 20-millisecond burns to the outer retina at 1 hour. C, Burns reduce in size and remain localized to the apical RPE after 4 weeks (arrows).

These autofluorescence and FD-OCT laser-tissue interactions were the same for all the patients studied.

Pascal 20-millisecond PRP burns may be graded into 4 stages: (1) the outer HRL remains intact, and foci of reduced reflectivity may be present in the outer HRL; (2) diffuse disruption and thickening of the outer HRL; (3) hyporeflexive splitting of the outer HRL, with compression of the vertical band of reflectivity in the outer plexiform layer/outer nuclear layer; and (4) a bleb of reduced optical reflectivity is present in the outer HRL, with elevation of the inner aspect and a triangular band of hyperreflectivity in the outer plexiform layer/outer nuclear layer (**Figure 3**).

The healing responses of 20-millisecond compared with 100-millisecond burns across time are shown in **Figure 4**. At 2 weeks, localized areas of hyperreflectivity in the outer HRL corresponded to laser burns, and these individual burns were associated with increased autofluorescence. The localized areas of hyperreflectivity at the level of the JI/OSP and the apical RPE persisted 4 weeks after treatment in the 20MS-PRP and 100SS-PRP groups (**Figure 5**). The healing responses observed with autofluorescence and FD-OCT across time were identical for each eye in the 20MS-PRP group.

The baseline predetermined laser burn size was 400 μm , and changes in laser burn sizes are shown in

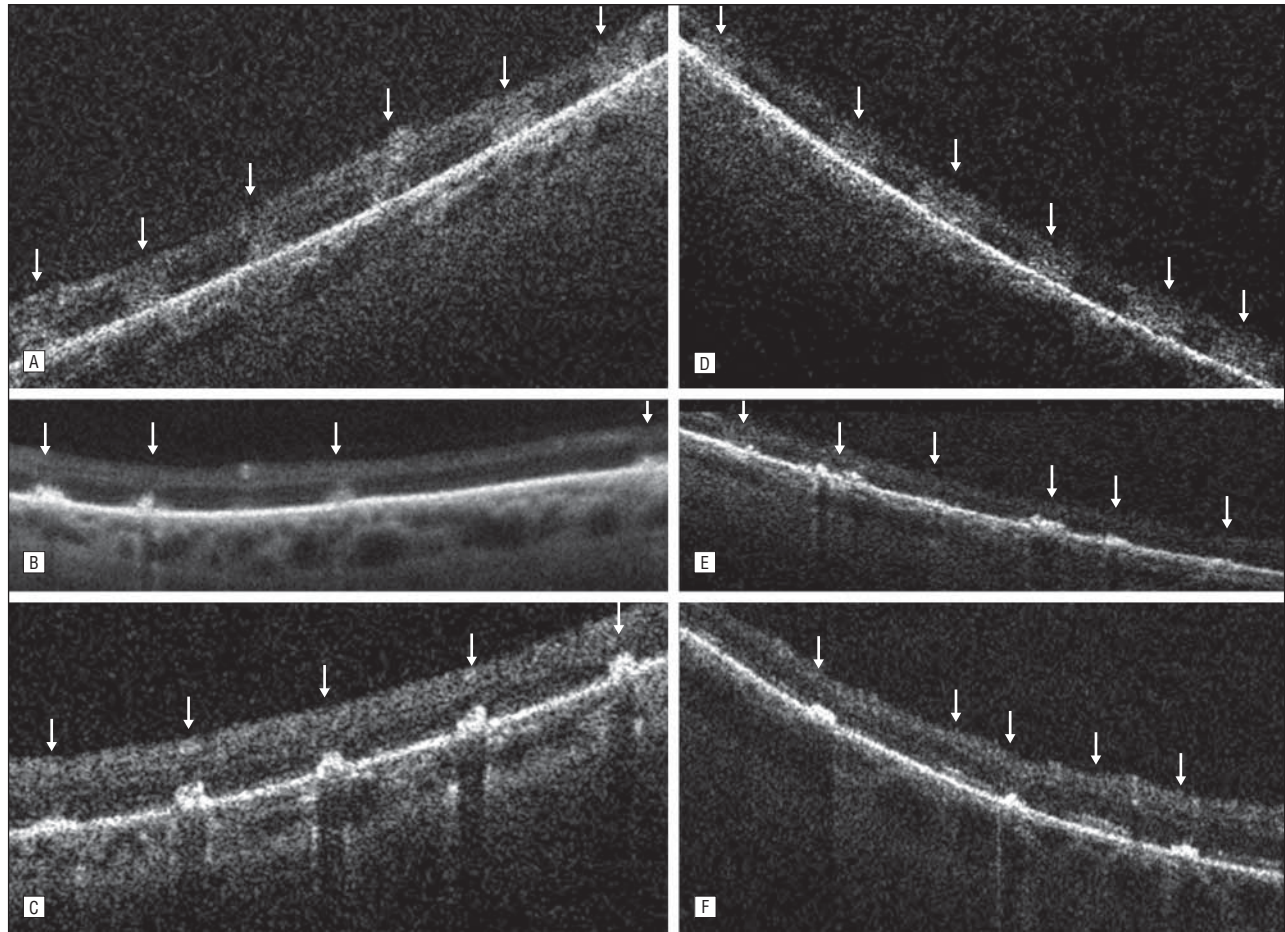


Figure 4. Arrows designate laser lesions at all time points. Fourier domain optical coherence tomography horizontal scans at 1 hour displaying similar vertical bands of increased reflectivity in the outer plexiform layer for both 20-millisecond burns (A) and 100-millisecond burns (D). The 20-millisecond burns show a triangular configuration in the outer plexiform layer at 2 weeks (B), with more diffuse thickening of the apical retinal pigment epithelium (RPE) produced with 100 milliseconds (E). There is increased pigmentation of burns after 4 weeks, and the 20-millisecond burns remain localized to the apical RPE (C) and the 100-millisecond burns produce more diffuse thickening of the apical RPE and the junction of the inner and outer segments of the photoreceptors (F).

Figure 6. The GLD was measured from autofluorescence images. At threshold 20MS-PRP, the mean (SD) GLD at 1 hour was 382 (15.4) μm (range, 357-396 μm). After 1 month, the mean (SD) GLD had reduced to 248 (13.9) μm (range, 224-266 μm). The size of 20-millisecond burns reduced by a factor of 35%, and this reduction was significant ($P < .001$). Pascal burns were columnar in shape, with hyporeflective zones between each burn (Figure 3). After 4 weeks, we observed that 20-millisecond burns remained highly localized, with no significant reflectivity changes in adjacent RPE cells and overlying neuroretina. The basal aspect of the outer HRL remained intact for 20-millisecond burns.

In contrast, the 100-millisecond burns appeared as more diffuse areas of hyperreflectivity in the JI/OSP and the apical part of the RPE across 4 weeks. At 1 hour, the mean (SD) GLD was 445 (16.4) μm (range, 418-469 μm), and there was no significant change in the size of the burns after 1 month, with a mean (SD) GLD of 446 (28.9) μm (range, 411-498 μm ; $P = .92$) (Figure 6). The patterns and intensity of autofluorescence and pigmentation were highly variable at 4 weeks, with varying sizes and shapes of burns.

Comparison of 20MS-PRP and 100SS-PRP burns at 1 hour and 4 weeks demonstrated significant differences in

laser burn sizes (Figure 6). At 1 hour, the difference in GLD was 63 μm (95% confidence interval, 50-75 μm ; $P < .001$). At 4 weeks, the difference had increased to 198 μm (95% confidence interval, 178-218 μm ; $P < .001$). Across time, progressive alterations in the morphologic features of Pascal burns depended on pulse duration and fluence.

COMMENT

To our knowledge, this study shows for the first time in humans that 20-millisecond burns allow the tissues to undergo a healing response that may not occur after standard-duration photocoagulation. We cannot predict whether it is the lesion intensity or the pulse-duration that results in this reduction in burn size. This healing response is associated with a significant reduction in burn size across time for 20-millisecond pulse duration Pascal, with no significant disruption to either the inner retina or the basal RPE. Higher-fluence 100-millisecond burns developed larger defects due to thermal blooming and collateral damage, with no alteration in burn size across time or any healing laser-tissue interactions using these imaging methods. At different pulse durations, fluence

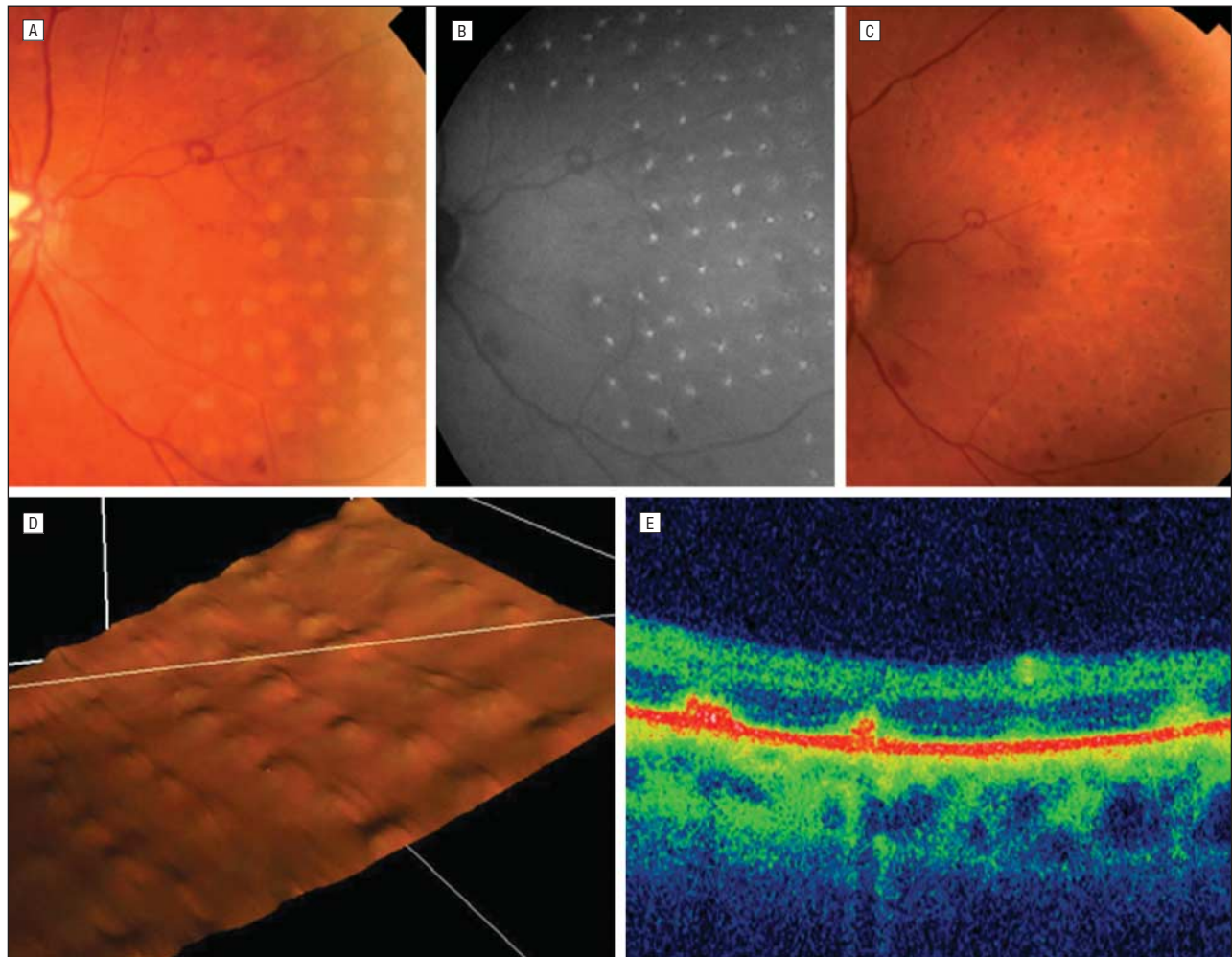


Figure 5. Imaging of Pascal 20-millisecond treatment burns (400- μm spot size) at 2 weeks. A, The laser burns are partially visible on color fundus photography. B, Autofluorescence at 4 weeks shows almost uniform hyperautofluorescent spots that correlate with central pigmentation of laser burns in the complete Pascal 5×5 array. C, After 4 weeks, the laser burns show increased pigmentation. D, Three-dimensional Fourier domain optical coherence tomography mapping demonstrates localization of 20-millisecond burns to the level of the junction of the inner and outer segments of the photoreceptors (JI/OSP) with no disruption at the level of the apical retinal pigment epithelium. White grid lines demonstrate the exact alignment of the retinal layers during 3-dimensional software analysis of the horizontal optical coherence tomography scans. E, The high-definition, overlapping radial scan demonstrates increased foci on the internal aspect of the outer highly reflective layer that corresponds to the JI/OSP.

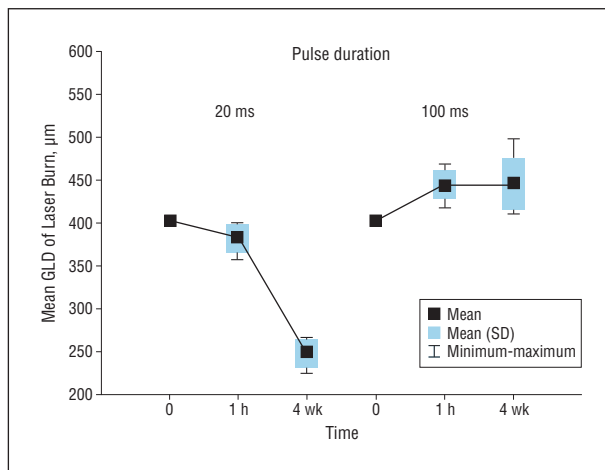


Figure 6. Variation in sizes of laser burns across time: Pascal 20- vs 100-ms pulse durations. The greatest linear diameters (GLDs) of laser lesions were measured from autofluorescence images. Aerial laser spot size is 400 μm for both groups, and this arbitrary measure has been marked at predetermined time 0.

may be titrated to achieve an optimal laser dosage and threshold burns in the outer retina, with healing of laser burns and minimization of photoreceptor injury.

The RPE shows cellular heterogeneity, and the melanosome numbers are variable in the RPE population in the retina.¹⁷ We observed different optical morphologic features for PRP burns. A graded series of optical effects were visualized at the level of the HRL for 20- and 100-millisecond pulse durations. Four grades of retinal injury were demonstrated in a single Pascal 5×5 array, using the same fluence and power to produce a threshold barely visible burn (Figure 3). A mild threshold burn is observed as a homogeneous apical RPE-JI/OSP coalescence effect, and this may progress to separation and edema in the outer HRL. As the outer HRL separates from the JI/OSP, there is increasing disruption of the apical RPE.

The histopathologic features of argon laser lesions have previously been correlated with time-domain OCT in *Macaca mulatta*.¹⁸ The laser-induced tissue changes ini-

tially after the laser occupied the full thickness of the retina, and the outer retina appeared to be the main site of scar formation with time. In a recent study, we¹⁶ demonstrated laser uptake at subvisible and visible laser intensity at 10 milliseconds. The present study has now evaluated the effects of 20-millisecond laser lesions compared with 100-millisecond lesions at different layers of the neuroretina-RPE complex.

Ultrashort pulse-duration photocoagulation in *Macaca* retina has demonstrated that the RPE may elevate and detach from the Bruch membrane.⁴ Fourier domain OCT demonstrated that laser photocoagulation effects on the tissue were localized to the JI/OSP and the apical RPE. At this stage, the hyporeflective bleb in the outer HRL may represent extensive vacuolation in the apical RPE cells. The cavitation alterations in the RPE may reflect increased absorption of laser energy by the melanosomes, with bubble formation around the melanin granules.¹⁹ This effect was not consistently observed in every laser burn, perhaps as a result of the varying extent of melanosome density in the outer retina.

Photocoagulation burns did not disrupt the basal RPE in any patient, as confirmed by 3D slicing on FD-OCT (Figures 1 and 2). The increased reflectivity signals that persist at the level of the JI/OSP at 2 weeks may represent photoreceptor migration toward and aggregation at the site of photocoagulation burns.⁶ We used autofluorescence imaging in this study to explain the reflectivity changes observed on FD-OCT.

It is well recognized that intracellular degenerations of the macula and retina may increase levels of lipofuscin in the RPE.^{20,21} Variations in autofluorescence patterns associated with 100-millisecond burns after 2 weeks suggest that a cascade of laser-tissue interaction changes may occur at the level of the outer HRL. Studies in murine models have demonstrated autofluorescence derived from perivascular and subretinal microglial cells. After laser photocoagulation, microglial cells migrate from the inner retina toward the site of the laser-induced retinal injury.²² We¹⁶ previously demonstrated 10-millisecond Pascal laser alterations at the level of the JI/OSP and the apical RPE with FD-OCT. Spatial correlation of thermal alterations in the RPE was previously demonstrated on autofluorescence.¹⁶ We¹⁶ showed that the low signal could be due to blockage of RPE autofluorescence by either thermal modifications or coagulation in the outer retina.

A potential explanation for laser burn healing responses may be related to fluence, calculated as (power \times time)/area. We demonstrated that the fluence required to produce a threshold ETDRS PRP burn on the retina is significantly lower for a pulse duration of 20 milliseconds compared with a conventional 100-millisecond duration. A lower fluence dosing of laser has been shown to result in fewer structural alterations in the outer retina.⁸ At shorter and longer pulse durations, the RPE absorbs the laser light and is killed, and at both pulse durations, the RPE proliferates to fill the area destroyed.⁸

Pascal 100-millisecond burns become more variable in size and shape with time, with partial coalescence of burns and variable hyperautofluorescent spots visible. In-

creased autofluorescent signals are more visible owing to resolution of the high reflectivity signal, previously observed on FD-OCT in the outer retina that had immediately blocked the normal autofluorescence. The 100-millisecond burns produced diffuse thickening of the JI/OSP and the outer HRL at 2 weeks, and this is thought to be because of greater heat diffusion in the outer retinal tissues. The 20-millisecond burns in the Pascal 5 \times 5 array appear as hyperautofluorescent spots of uniform size and shape in the immediate term.

The increased autofluorescence signals after PRP are derived from the increased load of lipofuscin sequestered by microglial proliferation. The direct microglial migration around melanosomes and toward the nidus of long-pulse burns may account for the variable patterns of hyperautofluorescence observed in these patients.⁸ There may be increased aggregation of microglia in the subretinal space with a longer pulse-duration laser because higher fluences may activate a larger population of microglia to migrate toward the 100-millisecond burns.^{22,23}

In the present patients, the microglial response to laser-induced injury may spread over a larger zone in the 100-millisecond burns. This response may explain the lack of reduction in the sizes of 100-millisecond burns across 4 weeks. However, 20-millisecond burns remain more uniform in shape on autofluorescence, and there is likely to be minimal disruption of lipofuscin by macrophage and microglial cell migration. At lower threshold fluences, the 20-millisecond burns significantly reduce in size with time, and this may be related to the healing of laser lesions in the outer retina. We showed that the dosing of laser treatment at different pulse durations may determine outer retinal injury and progressive enlargement of burns across time. We observed an increased the accumulation of lipofuscin at higher fluence levels, and this may lead to greater photoreceptor shortening and apoptosis across time rather than to a healing response. At longer pulse durations, there may be higher risk of peripheral scotomas and loss of scotopic visual function, especially after repeated PRP treatments in a patient's lifetime.

At 4 weeks, there were localized areas of hyperreflectivity at the level of the JI/OSP and the upper surface of the RPE that corresponded to 20-millisecond laser burns. The mean GLD of burns measured 152 μ m less than the original 400- μ m laser spot size. However, the size of the hyperreflective zone was enlarged after 100-millisecond PRP, with the mean GLD at 1 hour being significantly greater than that of the initial 20-millisecond burns. This increased alteration in the outer retina has been reported to result from greater thermal spread.⁸

In the short-term, the natural history of medium compared with longer pulse-duration burns toward establishment of laser photocoagulation scars is significantly different owing to the association of more collateral heat diffusion or thermal blooming to 100-millisecond burns.²⁴ The sizes of 100-millisecond burns at 4 weeks are associated with a higher standard deviation, and this confirms a larger variation in the final GLD of 100-millisecond burns. However, 20-millisecond burns are recorded with a lower standard devia-

tion at all time points, and this suggests more uniform and predictable healing responses of 20-millisecond burns across time.

In this study, the variation in laser lesion sizes has resulted in nonequivalent treatment areas. To achieve equivalent treated areas, calculate the area of the average lesion for 20- and 100-millisecond lesions to achieve the same treated area of retina rather than the same number of burns.

The present study results highlight the importance of using FD-OCT and autofluorescence to localize and monitor photocoagulation. It has been suggested that subretinal microglia at sites of laser injury may ultimately lead to RPE apoptosis and photoreceptor loss.²³ Autofluorescence imaging may be a useful tool for monitoring these cellular alterations across time. Autofluorescence imaging may prevent retreating previously treated areas and subsequently minimize PRP burn expansion. Limitations of this study should be understood in the context that the burn characteristics of 20- and 100-millisecond pulse durations have been made using a single power setting for each of the 2 pulse durations in this study. Also, it was beyond the scope of this study to correlate variations in the healing effects of the different laser variables with therapeutic effects.

These observations of laser-tissue interactions at different pulse durations suggest that laser PRP treatment should be considered in terms of laser dosage in the outer retina, and practitioners may titrate laser fluence for achieving threshold burns and healing responses for laser lesions in the outer retina.

Submitted for Publication: May 14, 2009; final revision received October 13, 2009; accepted October 19, 2009.

Correspondence: Paulo E. Stanga, MD, Manchester Royal Eye Hospital, Oxford Road, Manchester M139WH, England (retinaspecialist@btinternet.com).

Author Contributions: Mr Muqit had full access to all the data in the study and takes responsibility for the integrity of the data and the accuracy of the data analysis.

Financial Disclosure: Dr Marcellino is an employee of and Dr Stanga has received financial support from OptiMedica Corp.

Funding/Support: This study was supported by the National Institute for Health Research Manchester Biomedical Research Centre and OptiMedica Corp.

Role of the Sponsor: OptiMedica Corp had no role in the design and conduct of the study; in the collection, analysis, and interpretation of the data; or in the preparation, review, or approval of the manuscript.

Additional Information: This is a phase 1 study registered at: Research and Development Office, Trial Number: R00037, Central Manchester University Hospitals NHS Foundation Trust (<http://www.cmft.nhs.uk>).

1. Early Treatment of Diabetic Retinopathy Study Research Group. Techniques for scatter and local photocoagulation treatment of diabetic retinopathy: Early Treatment of Diabetic Retinopathy Study Report No. 3. *Int Ophthalmol Clin*. 1987; 27(4):254-264.
2. Stanga PE, Reck AC, Hamilton AM. Micropulse laser in the treatment of diabetic macular oedema. *Semin Ophthalmol*. 1999;14(4):210-213.
3. Framme C, Schuele G, Roider J, Birngruber R, Brinkmann R. Influence of pulse duration and pulse number in selective RPE laser treatment. *Lasers Surg Med*. 2004;34(3):206-215.
4. Toth CA, Narayan DG, Cain CP, et al. Pathology of macular lesions from subnanosecond pulses of visible laser energy. *Invest Ophthalmol Vis Sci*. 1997; 38(11):2204-2213.
5. Maeshima K, Utsugi-Sutoh N, Otani T, Kishi S. Progressive enlargement of scattered photocoagulation scars in diabetic retinopathy. *Retina*. 2004;24(4):507-511.
6. Paulus YM, Jain A, Gariano RF, et al. Healing of retinal photocoagulation lesions. *Invest Ophthalmol Vis Sci*. 2008;49(12):5540-5545.
7. Framme C, Brinkmann R, Birngruber R, Roider J. Autofluorescence imaging after selective RPE laser treatment in macular diseases and clinical outcome: a pilot study. *Br J Ophthalmol*. 2002;86(10):1099-1106.
8. Jain A, Blumenkranz MS, Paulus Y, et al. Effect of pulse duration on size and character of the lesion in retinal photocoagulation. *Arch Ophthalmol*. 2008; 126(1):78-85.
9. Blumenkranz MS, Yellachich D, Andersen DE, et al. Semiautomated patterned scanning laser for retinal photocoagulation. *Retina*. 2006;26(3):370-376.
10. Marshall J, Hamilton AM, Bird AC. Histopathology of ruby and argon laser lesions in monkey and human retina: a comparative study. *Br J Ophthalmol*. 1975; 59(11):610-630.
11. Stanga PE, Kychenthal A, Fitzke FW, et al. Retinal pigment epithelium translocation after choroidal neovascular membrane removal in age-related macular degeneration. *Ophthalmology*. 2002;109(8):1492-1498.
12. Sanghvi C, McLauchlan R, Delgado C, et al. Initial experience with the Pascal photocoagulator: a pilot study of 75 procedures. *Br J Ophthalmol*. 2008;92(8):1061-1064.
13. Delori FC, Dorey CK, Staurengi G, Arend O, Goger DG, Weiter JJ. In vivo fluorescence of the ocular fundus exhibits retinal pigment epithelium lipofuscin characteristics. *Invest Ophthalmol Vis Sci*. 1995;36(3):718-729.
14. Schmitz-Valckenberg S, Holz FG, Bird AC, Spaide RF. Fundus autofluorescence imaging: review and perspectives. *Retina*. 2008;28(3):385-409.
15. Leitgeb R, Hitzinger CK, Fercher AF. Performance of Fourier domain vs. time domain optical coherence tomography. *Opt Express*. 2003;11(8):889-894.
16. Muqit MM, Gray JC, Marcellino GR, et al. Fundus autofluorescence and Fourier-domain optical coherence tomography imaging of 10 and 20 millisecond Pascal retinal photocoagulation treatment. *Br J Ophthalmol*. 2009;93(4):518-525.
17. Pollack JS, Kim JE, Pulido JS, Burke JM. Tissue effects of subclinical diode laser treatment of the retina. *Arch Ophthalmol*. 1998;116(12):1633-1639.
18. Toth CA, Birngruber R, Boppert SA, et al. Argon laser retinal lesions evaluated in vivo by optical coherence tomography. *Am J Ophthalmol*. 1997;123(2):188-198.
19. Roider J, El Hifnawi ES, Birngruber R. Bubble formation as primary interaction mechanism in retinal laser exposure with 200-ns laser pulses. *Lasers Surg Med*. 1998;22(4):240-248.
20. Combadière C, Feumi C, Raoul W, et al. CX3CR1-dependent subretinal microglia cell accumulation is associated with cardinal features of age-related macular degeneration. *J Clin Invest*. 2007;117(10):2920-2928.
21. Gupta N, Brown KE, Milam AH. Activated microglia in human retinitis pigmentosa, late-onset retinal degeneration, and age-related macular degeneration. *Exp Eye Res*. 2003;76(4):463-471.
22. Xu H, Chen M, Manivannan A, Lois N, Forrester JV. Age-dependent accumulation of lipofuscin in perivascular and subretinal microglia in experimental mice. *Aging Cell*. 2008;7(1):58-68.
23. Lee JE, Liang KJ, Fariss RN, Wong WT. Ex vivo dynamic imaging of retinal microglia using time-lapse confocal microscopy. *Invest Ophthalmol Vis Sci*. 2008; 49(9):4169-4176.
24. Smith DC. High-power laser propagation: thermal blooming. *Proc IEEE*. 1977;65(12):1679-1714.